SURVEY AND ALIGNMENT FOR THE APS UPGRADE STORAGE RING*

W. G. Jansma†, C. L. Doose, J. S. Downey, R. C. Gwekoh, A. Jain, S. P. Jarvis, J. J. Nudell
Argonne National Laboratory, Lemont, IL, USA

Abstract

The Advanced Photon Source (APS) is a synchrotron X-ray facility located at Argonne National Laboratory, in operation since 1996. The APS recently completed an extensive upgrade, replacing the original APS electron storage ring with a state-of-the-art multi-bend achromat machine. The upgraded storage ring generates X-rays up to 500 times brighter than the original ring.

After more than 25 years of operation, the original APS storage ring was shut down on April 24, 2023, disassembled and removed. New, pre-assembled storage ring modules were installed, and the first electrons were injected into the new ring on April 13, 2024, less than one year later. The first stored electron beam was achieved on April 20, 2024.

In this paper we summarize the years of planning and preparation needed to successfully accomplish the goal replacing the 1,104-meter circumference storage ring within a one-year window. Magnet fiducialization, module assembly, survey control, and module installation and alignment will be presented.

BACKGROUND

Planning for the APS upgrade (APSU) began more than a decade ago and culminated in April 2024 with the successful startup of the upgraded storage ring. Stored beam was achieved within one week of the first injection of electrons. Preparation for the upgrade was driven by the ambitious goal to have the new storage ring back up and running within one year of shutting down the original APS. Years of effort went into preparation for the dark time. As far back as 2016 we were developing the magnet fiducialization process; the first APSU magnet was referenced in 2019, with the final magnet completed in 2023 – a four-year effort. Development of the alignment process for module assemblies began in 2019. The first module was assembled in 2021 in an off-site facility and the final module was completed in December 2023. Automated alignment processes were developed concurrent with these activities. The goal to start up the new APS storage ring within one-year of dark time was achieved.

ALIGNMENT REQUIREMENTS

Alignment tolerances for the APSU storage ring are stringent; assembly and installation tolerances are listed in Table 1, and a generic storage ring sector is depicted in Fig. 1. Note that two girder-to-girder tolerances are listed, 100 μm RMS for the alignment between DLM and FODO modules relative to a smooth long-wavelength curve, and a 50 μm RMS for the QMQ modules straddling between the DLM and FODO modules. The QMQ's will be aligned in such a way that Q6 is positioned relative to the DLM "geometry line" with less than 50-μm rms and 1.5-sigma cutoff, and Q7 will be placed the same way relative to the FODO "geometry line." Individual elements on the DLM and FODO girders will be aligned relative to the "geometry line" with 30-μm rms and a 2-sigma cutoff [1]. Maintaining alignment to these specifications will be a continuous effort throughout the life of the machine.

MAGNET FIDUCIALIZATION

Precision magnet fiducialization provides the foundation for achieving overall alignment results within the strict tolerance specification. The APS-U storage ring includes 1321 magnets aligned on 200 modules. Two rotating wire benches were utilized for multipole fiducialization [2], and a Hall probe bench was employed for dipole measurement [3].

The rotating wire measurement system was developed at the APS. We selected a rotating wire rather than a fixed wire because it is easier to precisely locate the rotation axis than it is to measure the location of a fixed wire. The system utilizes a BeCu taut wire loop stretched through the aperture of the magnet that rotates using synchronized stages, with one leg of the loop approximately on-axis, and the other leg rotating about the axis. The wire loop may be translated horizontally and vertically to place the rotation axis within 1-μm of the magnetic center. Field components are derived from Fast Fourier Transform (FFT) of induced voltage or flux, and the magnetic center is derived from the field components. A diagram of the rotating wire system is shown in Fig. 2.

The center of rotation is referenced using a laser tracker. 3D laser tracker coordinate data are taken with the rotation axis centered in X and translated vertically to compensate for the wire sag offset. The following points and features are measured from 2 laser tracker positions:

- Points at eight azimuthal positions of both wire holders in 45° increments
- Upstream and Downstream face planes of the magnet yoke
- The magnet base plane (Y reference)
- The machined –X side reference planes (X reference)
- Magnet fiducial nests and bench monuments

*This research used resources of the Advanced Photon Source, a U.S. Department of Energy (DOE) Office of Science user facility at Argonne National Laboratory and is based on research supported by the U.S. DOE Office of Science-Basic Energy Sciences, under Contract No. DE-AC02-06CH11357.

† jansma@anl.gov

Table 1: Survey and Alignment Assembly and Installation Tolerances

Parameter	Value	Units
Storage ring		
Circumference	30	mm
Source points		
Survey tolerance in ID source position (horiz. and vert.)	2.0	mm peak-to-peak
Global ring flatness (vert.)	4.0	mm peak-to-peak
M1 and M2 dipoles		
Positional misalignment	100	µm rms (2-sigma cutoff)
Pitch/yaw	0.1	mrad rms (2-sigma cutoff)
Modules		
Girder to girder (DLM to FODO)	100	µm rms (1-sigma cutoff)
Girder to girder (QMQ to DLM or FODO)	50	µm rms (1.5-sigma cutoff)
Elements within a module		
Magnet to magnet (M3/M4, quads, sexts)	30	µm rms (2-sigma cutoff)
Roll (M3/M4, quads, sexts)[a,b]	±2	mrad (repair threshold)
Pitch/yaw (M3/M4, quads, sexts)	0.7	mrad rms (2-sigma cutoff)
Longitudinal plinth placement tolerance	250	µm rms
BPM centroid mechanical offset allowance	250	µm rms
BPM roll	1	mrad rms (2-sigma cutoff)
Fast corrector longitudinal alignment allowance	±1	mm peak-peak
Booster to storage ring (BTS)		
Magnet to magnet	150	µm rms (2-sigma cutoff)
Quadrupole vibration (above 0.1 Hz)	1	µm rms

[a]Magnet roll about the axis defined by the particle beam's nominal trajectory is specified.
[b]Above this threshold, an attempt should be made to repair the roll angle
Revised: 12-19-2022 (SVN Rev.751)

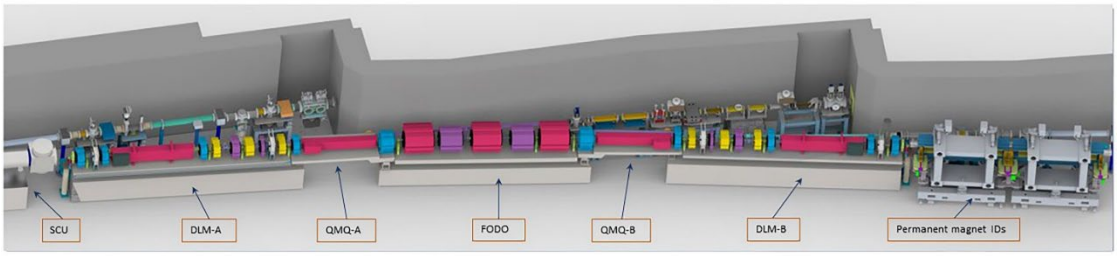

Figure 1: Generic APS-U storage ring sector.

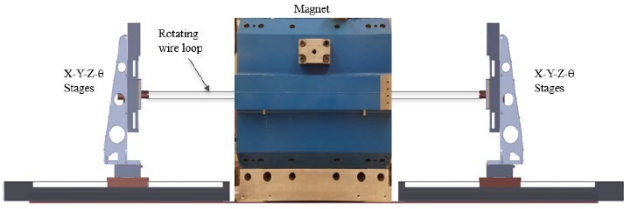

Figure 2: Rotating wire multipole measurement system.

Circles are fitted to the azimuthal points to establish radius points; a line constructed between the radii defines the rotation axis. The primary datum for the magnet coordinate frame is the magnet XZ base plane; the rotation axis orients Z. The origin is a point at the intersection of the magnet vertical XY mid-plane and the rotation axis, and represents the magnetic center. Note that some pitch may be present in the wire rotation axis. Uncertainty for the rotating wire measurement bench is 6-µm rms.

The Hall probe bench was utilized for fiducialization of the L-bend dipole magnets. This system translates a Hall probe and other sensors through the dipole field to characterize the field and define the vertex point within each magnet. The vertex point represents the intersection of the incoming and outgoing electron beam trajectories. The dipole magnets are pre-surveyed to establish the mechanical centers. The magnets are then placed on the Hall probe bench, and the mechanical center and orientation of the magnet are surveyed within the bench coordinate system. The vertex point derived from the magnetic measurements

is designated as the origin of the coordinate frame for the local mechanical survey fiducials to be used for alignment of the dipoles within the module assemblies.

Individual fiducial reports include comprehensive measurement records for each magnet. A compilation file includes fiducial data and horizontal / vertical reference plane information for all APS-U multipole and dipole magnets and is stored in the APS-U component database (CDB) for use during module assembly.

MODULE ASSEMBLY

The APS-U module assembly and alignment process was developed and tested beginning in 2019 [4]. Alignment of storage ring modules was completed in an off-site assembly and storage facility located approximately 5-km from the APS site. Early in the project the decision was made to rely on machining tolerances to achieve precision alignment of components within the module assemblies and increase efficiency in the assembly process.

Magnet Alignment

A multi-step, iterative process was developed to assemble the magnets into a nominal spatial arrangement. The APS has 40 storage ring sectors of the same geometry; each sector subtends 9 degrees of arc. The modules are interchangeable with respect to where they are to be installed in the ring, so a generic coordinate system valid for all storage ring sectors was utilized for the fiducial reporting frame. The process involved data acquisition, quality evaluation, analysis of data, generation of reduced coordinate files, automated point renaming and publication of traceability reports. The steps were automated to increase efficiency, ensure consistency, and reduce the possibility of error. The software platform integrates Spatial Analyzer (SA), Python/Jupyter Lab, Excel, Visual BASIC (VBA), and the CDB to streamline the process. SA is the primary metrology software tool utilized in the module alignment process. Sophisticated measurement plan tools were developed within SA to automate multiple measurement and data processing steps. SA's Unified Spatial Metrology Network (USMN) feature was utilized to bundle multiple laser tracker stations for the module surveys and for final module assembly fiducialization.

The magnet compilation file in the CDB includes 3-D coordinates of fiducials and measured reference surface distances for magnet shim calculations. Each magnet has a unique QR code linked to the CDB; when an array of magnets was staged for installation, the QR code for each magnet was scanned to populate a unique CDB page for the module. Custom Python applications reference the CDB module page to retrieve the data, transform and rename the local magnet fiducial coordinates into the ideal alignment lattice, and compute an optimized shim prescription for magnet-to-magnet alignment based on the *a-priori* reference data. No adjustment system was provided—vertical alignment (Y), pitch and roll are set against the girder plate surface; horizontal alignment (X) and yaw are set against locating stop blocks pinned to the girder surface. Locating pins in the plate set the magnet Z (longitudinal) positions. The girder material is cast iron; top surface flatness for the 5-m-long DLM and FODO modules is < 20 μm. Magnets were mounted and aligned on the cast-iron plate using the prescribed shim packs to align the X and Y positions. A laser tracker survey was performed, the surveyed magnet positions were analyzed to derive the magnetic centers, and if necessary, a second shimming iteration was carried out to improve magnet-to-magnet alignment. A comprehensive survey of the module was performed once the magnet-to-magnet alignment was within the specified tolerance. A global fit to all fiducials in all magnets on a module often resulted in a small systematic yaw and/or pitch of the derived magnet centers in the final fitted frame. This was perhaps a result of a global fit of fiducials in all magnets which individually had random yaw and pitch errors relative to placement in an ideal lattice. This did not really affect the quality of magnet-to-magnet alignment, but the module could be better placed in installation by slightly adjusting the yaw and pitch of the module frame. A second best-fit of the derived magnet centers only was therefore carried out to minimize the error in the magnetic center positions. Since the magnetic centers in a module lie on straight line segments with very small angles between segments, the roll is not very well determined during this fit. The roll was therefore constrained to zero during this second fit and only yaw and pitch were adjusted. This ensured that the module was installed with minimal offsets of all magnetic centers. Magnet alignment results were recorded in the CDB.

Excellent alignment results were achieved; well within the APS-U specification. Least-squares best-fit results for individual magnet offsets from their ideal position for a typical DLMA module is shown in Table 2.

Vacuum and Diagnostic Systems

The vacuum system relies on the precisely aligned magnet positions and machining tolerances to reduce the amount of effort in placing the components. The magnet alignment tolerance of 30-μm rms makes it possible to use features on the split magnets, e.g., pole tips and planar surfaces, as alignment reference features. Fiducial points on the lower magnet yokes and cast-iron plates provided reference points for measurement using a PCMM arm.

Locating pins in the girder plate surface were incorporated to precisely align the machined beam position monitor (BPM) supports to within 100 μm at installation with no further adjustment needed. The image in Fig. 3 shows a BPM assembly aligned against the locating pins on a module. Many vacuum connections are easier to make up *ex situ* on a bench rather than *in situ* within the module assembly where the space between magnets is tight. Sub-assemblies of multiple vacuum components were pre-aligned both to minimize exposure to atmosphere, and to increase efficiency in assembly. The image in Fig. 4 shows one of the vacuum system sub-assemblies. The flange connections in the middle of the sub-assembly are very difficult to make up *in situ*.

Table 2: Typical Least-Squares Best-Fit Result for a DLMA Module

Magnet	dX (mm)	dY (mm)	dZ (mm)	Pitch (mr)	Yaw (mr)	Roll (mr)
AQ1_0	0.001	-0.003	-0.180	-0.059	0.136	-0.009
AQ2_0	0.007	0.003	-0.076	-0.064	-0.129	-0.042
AQ3_0	0.000	0.005	0.058	-0.078	0.084	0.063
AS1_0	0.003	0.004	0.037	-0.019	0.185	0.009
AQ4_V	-0.011	-0.008	-0.007	-0.080	0.231	-0.001
AS2_0	0.000	-0.004	0.085	-0.099	0.006	0.000
AQ5_V	-0.007	-0.009	0.033	-0.032	0.019	0.000
AS3_0	-0.010	-0.005	0.066	-0.099	0.194	-0.101
Average	-0.002	-0.002	0.002	-0.066	0.091	-0.010
Std. Dev.	0.006	0.006	0.083	0.072	0.145	0.045
ABS Max	0.011	0.009	0.180	0.099	0.231	0.101

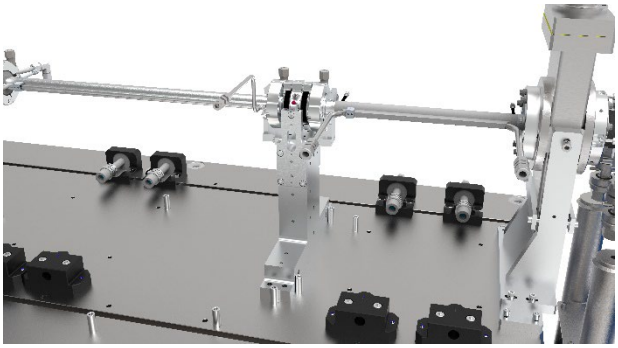

Figure 3: BPM assembly aligned against locating pins on a module.

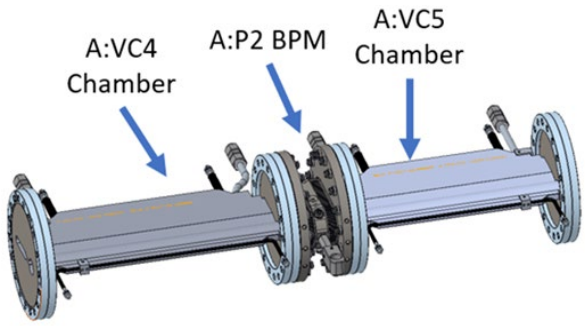

Figure 4: Vacuum system sub-assembly with two chambers and a BPM.

A portable coordinate measurement machine (PCMM) arm is utilized for alignment of the vacuum system; the pre-surveyed fiducials on the magnets and girder plate serve as the reference features.

SURVEY CONTROL NETWORK

In July 2023, immediately upon removal of the original storage ring, a new control network was established in the empty tunnel. The original network was densified with additional monuments. The absence of a machine in the tunnel provided a wider aspect ratio for measurement of the network than was possible during operations; instruments could be set up in the footprint of the old machine. A total of 1296 monuments were measured from 240 laser tracker positions. Temperature control was limited due to concurrent installation activities; doors to the outside were frequently opened. The network was measured over the course of three weeks by a crew of two technicians using one Leica AT403 laser tracker. Network adjustment was accomplished using NETOBS software developed at the Facility for Rare Isotope Beams (FRIB) at Michigan State University [5]. Eight datum points from the original survey were defined as a priori weighted control coordinates for the adjustment. Results showed the average point uncertainty was 31 μm, with a maximum uncertainty of 59 μm.

After adjustment, the network was translated to best-fit existing infrastructure based on original layout marks on the floor of the tunnel.

The storage ring control network serves as the primary control for the facility. Multiple secondary control networks have been established for the experiment hall that are tied directly to the primary storage ring network. Secondary networks are adjusted in SA using USMN, and best-fit to primary control using least-squares transformation. Currently we have placed >5,500 monuments for secondary networks.

We have detected motion in some areas of the tunnel infrastructure due to seasonal temperature variance. Monuments located adjacent to cold joints in the concrete tunnel structure move closer together in warm weather, and further apart in cool weather, indicating expansion and contraction of the tunnel segments. The magnitude is approximately 100 – 200 μm, primarily in the longitudinal (Z) direction. These areas will be closely monitored going forward.

Plans to perform a smoothing survey in August-September 2024 were postponed until December 2024 to focus effort on x-ray beamline realignment. We anticipate the need for realignment of some areas of the storage ring in 2025 based on the results of the December smoothing survey.

INSTALLATION AND ALIGNMENT

Preliminary Decisions

The original installation goal was to align the APSU machine along the old APS storage ring profile to meet existing beamline infrastructure and minimize the need for beamline realignment. This goal was abandoned after much consideration in favor of aligning the machine to the ideal design lattice. The decision was driven by the results of a final survey of the original APS storage ring in 2021. The survey revealed a 16-ppm scaling error in the machine alignment, resulting in the circumference of the old ring being 17-mm longer than specified, confirmed by radio frequency (RF) measurements taken by operations. In addition, the radial and vertical alignment deviated by as much as 5-mm around the ring. The decision to align to the ideal lattice simplified storage ring alignment and produced a higher-quality machine; however, beamline realignment effort was significantly increased.

Like the module assembly strategy, survey and alignment processes for module installation were extensively automated. Data acquisition, quality evaluation, analysis of data, generation of reduced coordinate files, and publication of reports were all scripted to ensure quality and consistency. Except for a few special modules, all the accelerator module types were interchangeable. Any module could be installed in any sector. Automated point renaming based on the installed location was employed. Scripting and automation played a key role in making it possible to install the new machine within a one-year window.

Layout

Layout of storage ring components and anchor bolt holes began upon completion of the survey network. Laser trackers were employed for layout of all points. Aluminum templates were utilized for common hole patterns that repeated across many sectors. Templates were composed of several segments that fit together like puzzle pieces to simplify moving them around and reduce weight. Non-templated points were laid out using SMR's in pin nest holders, with transfer punches the same diameter as the pins. More than 3,000 individual points were laid out prior to installation.

Plinth Installation

The first modules to be installed in the tunnel were the DLMA, DLMB and FODO types. These modules rest on large steel reinforced concrete bases, or plinths. Fully assembled plinth modules weigh approximately 20,000-kg, the FODO modules having the largest mass. There are 120 plinth modules, 40 of each type.

The plinth modules were transported on steel rollers and moved into rough position using a hydraulic dolly. Once in rough position, steel "end-riggers" were fastened to the ends of the plinth bases, and an A-frame hydraulic lift and adjustment system was pinned to the end-riggers. An image of the A-frame system is shown in Fig. 5, and an end rigger mounted to a plinth is seen in Fig. 6. The A-frames were used to lift the plinths off the rollers for removal, and to align the plinths into the final position. The plinths were aligned using a laser tracker oriented to the control network, using hydraulic assist for vertical adjustment and pusher bolts for horizontal adjustment. The end riggers were equipped with leveling feet; when the plinth bases were aligned to within +/- 1-mm the load was transferred on to the leveling feet and the A-frames were removed.

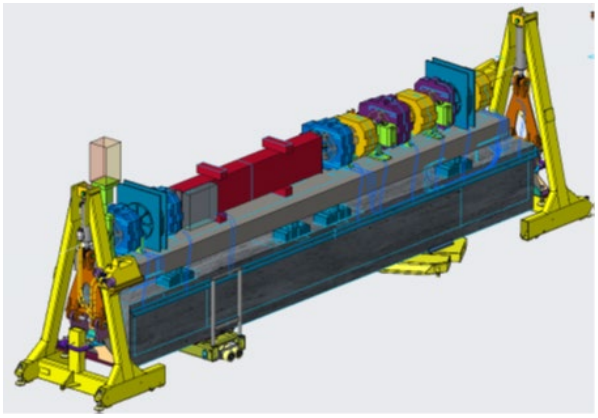

Figure 5: A-frame hydraulic lift and adjustment system.

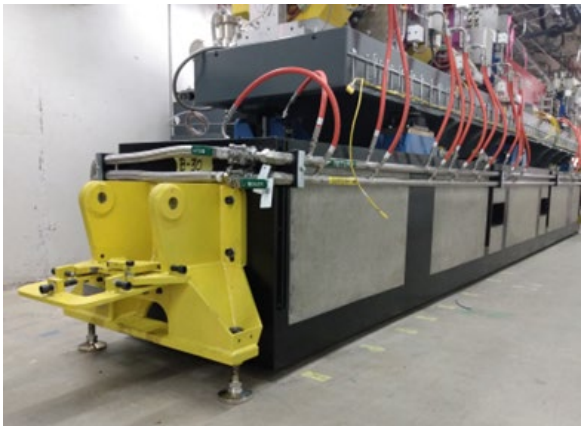

Figure 6: Plinth end rigger support for module for grouting.

Grout dams were installed at the base perimeter and epoxy grout was poured to fill the voids under the plinths. After the grout cured for 24 hours the dams and were removed and the load was transferred from the end riggers on to the grout. Note that there is no point loading under the plinths – they are supported by grout alone.

Fine alignment of upper module assemblies is performed after the grout cures and is discussed in the next section.

Module Alignment

With the plinths grouted in place, the upper DLMA, FODO and DLMB modules were aligned. The magnet arrays were pre-aligned during assembly, enabling the entire upper module assembly to be aligned as a single unit. The cast-iron surface plates supporting the pre-aligned magnet arrays are adjustable in six degrees of freedom (6-DoF) in a semi-kinematic arrangement with minimal constraint. Three vertical adjusters align elevation (Y), pitch and roll; two horizontal adjusters align transverse (X) and yaw, and one horizontal adjuster aligns the longitudinal (Z) position. The diagram in Fig. 7 shows the upper module adjustment system. All six adjustment mechanisms are wedge jacks

equipped with Belleville spring washers to pre-load the system and minimize alignment backlash. A diagram of the adjustment mechanisms is shown in Fig. 8. The intent is to treat the modules as rigid bodies; however, we encountered a minor problem with vertical coupling from horizontal adjusters. Slight deformation of the cast iron plate (<120 μm) was observed in a small percentage of the modules. The problem stems from misaligned spherical washers in the horizontal adjusters. The misalignment introduces coupling to the vertical direction. A solution to the coupling issue has been developed and will be implemented in future realignment efforts. The effect of the coupling on overall magnet to magnet alignment is minimal.

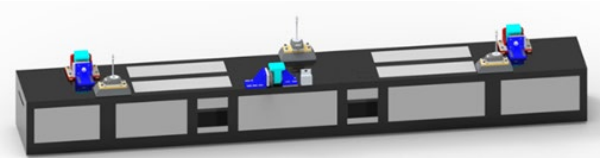

Figure 7: Upper module adjustment system.

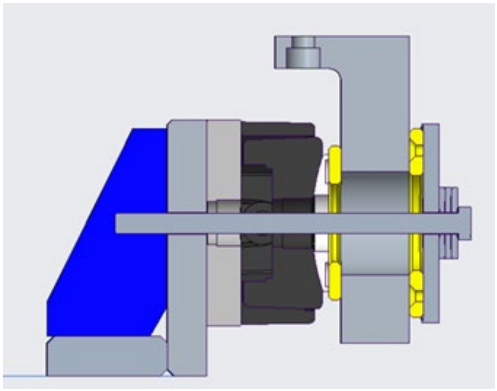

Figure 8: Wedge jack adjuster equipped with Belleville spring washers to pre-load the system and minimize alignment backlash

After the plinth modules were aligned the QMQA and QMQB modules were installed. These smaller modules bridge the DLM and FODO modules, resting on their plinth bases. The QMQ modules utilize the same adjustment hardware as the larger modules. The diagram in Fig. 1 shows a complete sector with all modules installed. A fully aligned DLMB module is shown in Fig. 9.

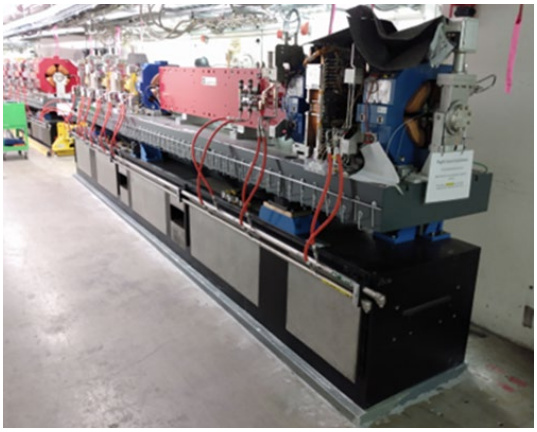

Figure 9: Fully aligned DLMB module.

Completed sectors are surveyed after all modules are aligned. Analysis and reporting of alignment results are automated processes, ensuring consistent results are recorded for all sectors.

Results

The final module was installed and aligned in March 2024; the results presented are the surveyed positions of the best-fit individual magnet centers as surveyed within the 2023 control network at the time of installation. A complete smoothing survey was scheduled for August 2024, but was postponed until December to focus effort on beamline realignment.

Installation survey results show radial magnet alignment to be 19-μm rms, with a maximum error of 101 μm. Vertical alignment is 30 μm rms, with a maximum error of 184 μm. Diagrams of the radial and vertical alignment results are shown in Figs. 10 and 11, respectively.

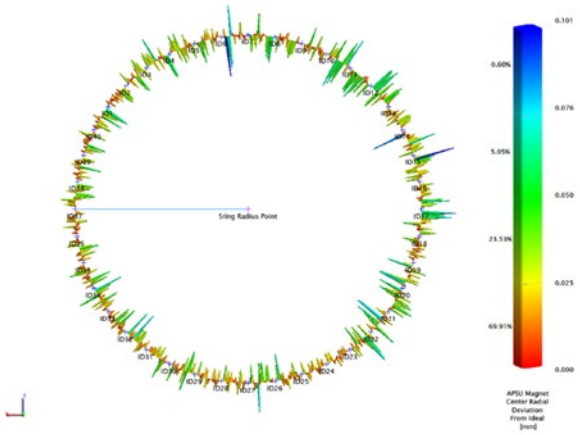

Figure 10 : APSU storage ring radial alignment [mm].

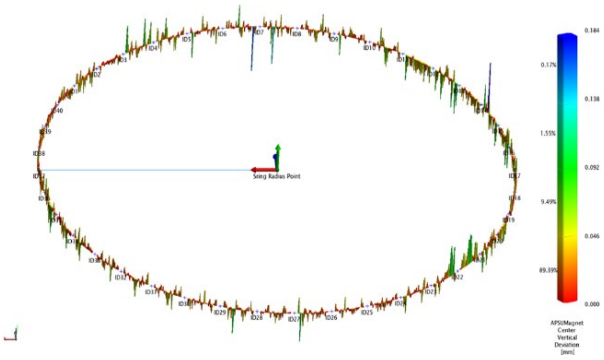

Figure 11: APSU storage ring vertical alignment [mm].

The ring circumference is difficult to calculate from survey data as it is not a circle, but a 520-sided irregular polygon, and is better described as “beam path length”, or “*s*” in the physics lattice. The value of *s* is determined by the radio frequency (RF) of the machine and provides independent verification of alignment quality.

The formula to calculate the beam path length (*s*) based on RF is:

$$s = \frac{c}{f} * n$$

where

c = speed of light (299,792,458 meters / second)
f = rf frequency
n = number of rf buckets = 1296 for the APS storage ring

Beam path length calculations based on the design and measured frequencies are shown in Table 3.

Table 3: APS Storage Ring E-beam Frequencies and Path Lengths

Criteria	Value	Units
Design frequency (f_{design})	352.055	MHz
Measured frequency (f_{meas})	352.054738	MHz
Design length (s_{design})	1,103.608884	meters
Measured length (s_{meas})	1,103.609699	meters
Δ_{length} ($s_{meas} - s_{design}$)	0.000815	meters

Measured "s" is only 0.82-mm from the design value; 0.74-ppm over the ~1,104-m storage ring circumference.

While still in the commissioning phase, storage ring emittance measurement, conducted at 50 milliamps of beam current, leads to an emittance of 45 picometers-radians (pm.rad). For certain configurations of the APS, such as round beam mode, the emittance is as low as 28 pm.rad. This emittance measurement is comfortably the best (meaning lowest) in the world for synchrotron X-ray facilities. The previous record, held by the Extremely Brilliant Source (EBS) at the European Synchrotron Radiation Facility (ESRF), is 134 pm.rad. [6]

CONCLUSION

The extraordinary results achieved by the APS survey and alignment team were the product of years of planning and preparation by a dedicated team of engineers and technicians. Laurent Chapon, director of APS, stated "It's exciting not just for our team, who worked hard to imagine, design, engineer, build and commission the new storage ring, but also for the entire light source community and the scientists who will make use of the brighter beams for decades to come to positively impact science and society." [6] The APS survey and alignment team is honored to have contributed to this great success story; we look forward to a bright future for the renewed APS.

ACKNOWLEDGEMENTS

The authors sincerely thank all who contributed to this work: Venus Apantenco, Nemanja Arsic, Dusan Banjanac, Alex Bolton, James Brown, Dino Canchola, Will Evans, Jason Hoffmeister, Cody Holz, Roberto Lopez, Kris Mietsner, Tommy Parchem, Davor Pavlovic, Scott Petersen, Spiro Skiadopoulos; Davide Bianculli, Josh Downey, Mark Erdmann, Rex Green, Rolando Gwekoh, Scott Izzo, Keith Knight, John Quintana, and many others. Special thanks to Peter Manwiller of the Facility for Rare Isotope Beams (FRIB), Michigan State University.

REFERENCES

[1] Photon Source Upgrade Accelerator Functional Requirements Document (FReD)," Argonne National Laboratory, Lemont, IL, USA, APSU_1695659, May 10, 2023.

[2] S. J. Izzo, C. L. Doose, A. K. Jain, and W. G. Jansma, "Magnet Measurement Systems for the Advanced Photon Source Upgrade," in Proc. MEDSI'20, Chicago, USA, Jul. 2021, pp.269. doi:10.18429/JACoW-MEDSI2020-WEPB03

[3] C. Doose, A. Jain, W. Jansma, M. Jaski, S. Izzo, R. Lopez, S. Skiadopoulos, and V. Apantenco, "The Hall Probe Measurement System for the Advanced Photon Source Upgrade Dipole Magnets," presented at the 22nd International Magnetic Measurement Workshop (IMMW22), Campinas, Brazil, Sep. 2022 (Virtual), https://pages.cnpem.br/immw22/

[4] K. J. Volin et al., "Magnet Module Assembly for the APS Upgrade," in Proc. MEDSI'20, Chicago, USA, Jul. 2021, pp. 283. doi:10.18429/JACoW-MEDSI2020-WEPB07

[5] P. E. Manwiller, "Three-Dimensional Network Adjustment of Laser Tracker Measurements for Large-Scale Metrology Applications," J. Surv. Eng., vol. 147, no. 1, Feb. 2021. doi:10.1061/(asce)su.1943-5428.0000332

[6] Advanced Photon Source achieves world-record electron beam emittance measurement, https://aps.anl.gov/APS-News/2024-08-23/advanced-photon-source-achieves-world-record-electron-beam-emittance